Inorganic Chemistry

Article

pubs.acs.org/IC

In Vitro Multiwavelength PDT with ^{3}IL States: Teaching Old Molecules New Tricks

Huimin Yin, Mat Stephenson, Jordan Gibson, Eric Sampson, Ge Shi, Tariq Sainuddin, Susan Monro, and Sherri A. McFarland*

Department of Chemistry, Acadia University, 6 University Avenue, Wolfville, Nova Scotia B4P 2R6, Canada

Supporting Information

ABSTRACT: The purpose of the present investigation was to ascertain whether ^{3}IL excited states with microsecond lifetimes are universally potent for photodynamic applications, and if these long-lived states are superior to their ^{3}MLCT counterparts as *in vitro* PDT agents. A family of blue-green absorbing, Ru(II)-based transition metal complexes derived from the π-expansive dppn ligand was prepared and characterized according to its photodynamic activity against HL-60 cells, and toward DNA in cell-free media. Complexes in this series that are characterized by low-energy and long-lived ^{3}IL excited states photocleaved DNA with blue, green, red, and near-IR light. This panchromatic photodynamic effect translated to *in vitro* multiwavelength photodynamic therapy (PDT) with red-light cytotoxicities as low as 1.5 μM (EC_{50}) for the parent complex and 400 nM for its more lipophilic counterpart. This potency is similar to that achieved with Ru(II)-based dyads containing long-lived ^{3}IL excitons located on appended pyrenyl units, and appears to be a general property of sufficiently long-lived excited states. Moreover, the red PDT observed for certain members of this family was almost 5 times more potent than Photofrin with therapeutic indices 30 times greater. Related Ru(II) complexes having lowest-lying ^{3}MLCT states of much shorter duration ($\leq$1 μs) did not yield DNA photodamage or *in vitro* PDT with red or near-IR light, nor did the corresponding Os(II) complex with a submicrosecond ^{3}IL excited state lifetime. Therefore, metal complexes that utilize highly photosensitizing ^{3}IL excited states, with suitably long lifetimes ($\gg$ 1 μs), are well-poised to elicit PDT at wavelengths even where their molar extinction coefficients are very low (<100 M^{-1} cm^{-1}). Herein we demonstrate that such unexpected reactivity gives rise to very effective PDT in the typical therapeutic window (600−850 nm).

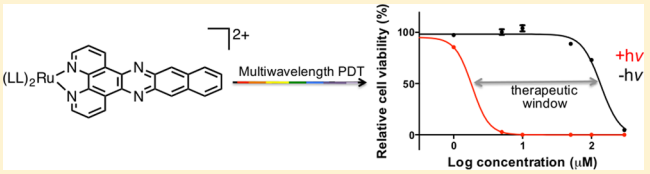

1. INTRODUCTION

1.1. Limited Success of Clinical PDT. Photodynamic therapy (PDT) is a promising strategy for treating cancer whereby light is used to activate an otherwise nontoxic prodrug, a photosensitizer (PS), in order to destroy tumors and tumor vasculature and to induce an immune response. Following photoactivation, the PS delivers a toxic burst of reactive oxygen species (ROS) that is confined spatially and temporally to the irradiated region, thus targeting malignant tissue while sparing healthy tissue. It is generally accepted that the principal mediator of biological damage in PDT is cytotoxic singlet oxygen ($^1\Delta_g$), produced via energy transfer in a type II photoprocess from the excited PS to ground state molecular O_2 ($^3\sum_g^-$).[1] However, other ROS and reactive intermediates generated through type I electron transfer processes can also play an important role, depending on the nature of the PS employed. As a concept PDT is highly selective, extremely potent, fast-acting, and very broad in scope. It combines all of the advantages of targeted therapy (without the cost) with the breadth and scope of classical chemotherapy (without the side effects). Unlike radiation treatment, it can be repeated many times, alone or in combination with other therapies. As such, PDT represents a powerful alternative, whether as a frontline or as an adjuvant therapy, while offering the opportunity to avoid the debilitating, dose-limiting side effects of chemotherapy and radiation.

Notwithstanding the enormous potential of PDT, it remains largely undeveloped in the 40 years since its first use in clinical oncology, except in a select number of highly specialized fields such as dermatological oncology and opthamology.[2−5] Plaetzer and coworkers have put forth convincing arguments to account for the absence of PDT in mainstream cancer treatment: (i) a lack of dosimetric control in clinical PDT, (ii) a longstanding PS-based approach to drug design for PDT, and (iii) the absence of detailed protocols for clinicians.[3] These factors have led to inadequate tumor response and unacceptable complications in the many attempts to use PDT in the clinic.[6−9] The unrealistic search for an *ideal* PS has compounded the inherent problem of proper dosimetry that arises from the complexity of the PDT mechanism itself,[3,10] and the result is an explosion of reported PSs for PDT in the primary literature with almost no corresponding advancement in the number of clinically approved PDT agents or consistent and successful clinical outcomes. These gaps are perpetuated by the tendency to develop PSs without considering a defined clinical indication

Received: January 29, 2014
Published: April 11, 2014

   dx.doi.org/10.1021/ic5002368 | *Inorg. Chem.* 2014, 53, 4548−4559

(tumor/tissue type) and in isolation from end users (clinicians).

Failure to realize the full potential of PDT is due, at least in part, to the large inter- and intratreatment variations in (i) PS pharmacokinetics and distribution, (ii) tissue optics, (iii) tissue oxygenation, and (iv) the dynamic interactions between these properties during PDT. With existing clinically approved PSs, it has been suggested that personalized dosimetry[8,11,12] may be the only strategy for reducing inter- and intratreatment variability, thus improving treatment outcomes. Unfortunately, current technology cannot achieve accurate quantification of nor precise control over the complexities of *in situ* clinical PDT dosimetry. We, therefore, propose that broadly versatile PSs could offset the problems associated with highly inconsistent and often compromised dosimetry of the PS, light fluence, and oxygen supply in tumors. Such agents must necessarily be able to exert strong PDT effects regardless of oxygen tension, with variable wavelengths of light and fluence rates. Their adaptability may prove useful in treating a wider range of tumor phenotypes with a single PS, eliminating the need to develop a new PS for each clinical indication, which is prohibitively expensive.

1.2. Versatile ^{3}IL States for Multiwavelength PDT. Metal-based coordination complexes related to $[Ru(bpy)_3]^{2+}$ are of considerable interest owing to their favorable absorption, photophysical, and electrochemical properties.[13] They are rivalled only by porphyrin and metalloporphyrins as active components in supramolecular systems for photoinduced energy and electron transfer.[14] Although the lifetimes of the triplet metal-to-ligand charge transfer (^{3}MLCT)-based excited state of $[Ru(bpy)_3]^{2+}$ and its many derivatives are relatively long at 1 μs (deoxygenated solution at room temperature), they are still too short for many luminescence-based applications. Castellano[15,16] and others[14,17] have exploited low-lying triplet intraligand (^{3}IL) excited states to achieve longer excited state lifetimes in Ru(II) polypyridyl complexes, thus making them much more attractive as PSs in optoelectronics and luminescence-based technologies. Importantly, we have shown that these states are also well-suited for photobiological applications such as PDT.[10,18]

Ford and Rogers[19] pioneered the concept of appending organic chromophores to polypyridyl ligands in order to prolong excited state lifetimes in Ru(II) coordination complexes. These original dyads were bichromophoric arrangements, with ligand-localized ^{3}IL states in equilibrium with the well-characterized ^{3}MLCT states. The resulting lifetimes were 10-fold longer (>10 μs) than those of traditional $[Ru(bpy)_3]^{2+}$-type complexes. Various derivatives of these early systems have produced lifetimes in excess of 150 μs by positioning the lowest-lying ^{3}IL state well below the lowest-lying ^{3}MLCT state.[14−16] We have also achieved pure lowest-lying ^{3}IL states in related complexes of $[Ru(bpy)_2(LL)]^{2+}$, where LL = 3-, 4-, or 5-(pyren-1-ylethynyl)-1,10-phenanthroline (3-, 4-, or 5-PEP), and the lifetimes range from 22 μs with 4-substitution on the 1,10-phenanthroline (phen) ring to 240 μs with 5-substitution in fluid solution at room temperature.[10] Despite a 10-fold span in lifetime in this series and $^1O_2$ quantum yields that vary from 65% to 87%, all three dyads are comparably potent *in vitro* PDT agents with light cytotoxicities in the nanomolar regime at low light fluence. Such systems are far more sensitive to excited state quenching by molecular oxygen (and other species) compared to traditional type II PSs. It follows that pure ^{3}IL states, characterized by very low radiative (k_r) and nonradiative (k_{nr}) rates that lead to suitably long lifetimes, should represent a general approach to achieving potent PDT with a large therapeutic window. Moreover, the extraordinary efficiency of the PDT effect for these PSs indicates that the wavelength range for photoactivation could be much broader than expected.

To test these assertions, we chose to explore the *in vitro* potency of ^{3}IL states derived from other constructs, namely π-expansive ligands that are contiguously fused as opposed to spatially separated polycyclic aromatic chromophores appended to diimine ligands. Turro and Thummel have shown that complexes of $[Ru(tpy)_n(pydppn)_{2-n}]^{2+}$ (n = 0,1), where pydppn =3-(pyrid-2′-yl)-4,5,9,16-tetraaza-dibenzo[*a*,*c*]-naphthacene, possess low-lying LC $^3\pi\pi^*$ states with lifetimes that exceed 20 μs and sensitize $^1O_2$ with 100% efficiency.[20] Foxon and coworkers[21,22] reported that bidentate complexes of Ru(II) containing a dppn ligand (dppn = benzo[*i*]dipyrido[3,2-*a*:2′,3′-*c*]phenazine) also possess low-lying, long-lived LC $^3\pi\pi^*$ states, and Turro[23] demonstrated the effectiveness of such systems as type I/II PS for DNA photocleavage and predicted their utility as PDT agents. To our knowledge, *in vitro* PDT with this series was not subsequently explored although the photodynamic inactivation (PDI) of *E. coli* by $[Ru(bpy)_2dppn]^{2+}$ has been reported.[24] The detailed photophysical and DNA interaction studies made available by these two groups for complexes containing the π-expansive dppn ligand[21−23,25] provide an excellent starting point for assessing the generality of *in vitro* PDT with ^{3}IL states.

The goal of the present study was to ascertain whether ^{3}IL states afforded by π-expansive ligands lead to potent PSs for *in vitro* PDT (in comparison to the previously reported PEP complexes[10,18]). We were particularly interested in whether ^{3}IL excited states with microsecond lifetimes are universally potent for photodynamic applications, and if these long-lived states are superior to their ^{3}MLCT counterparts as *in vitro* PDT agents. We hypothesized that the potency of ^{3}IL states might enable PDT with wavelengths of light for which molar absorptivities are very low. In other words, it should be possible —at least in principle— to stimulate these reactive ^{3}IL states with red and possibly near-IR light, giving rise to what we term *multi-wavelength* PDT. The ability to employ blue, green, red, or near-IR light —sequentially, simultaneously, or independently— for PS activation would greatly expand the utility and scope of a single PS for PDT, possibly mitigating the problems with *in vivo* dosimetry and reducing the large inter- and intratreatment variations that compromise clinical outcomes for PDT.

2. EXPERIMENTAL PROCEDURES

2.1. Materials. 2,2′-Bipyridine (bpy), 4,4′-dimethyl-2,2′-bipyridine (dmb), 4,4′-di-*t*-butyl-2,2′-bipyridine (dtbb), 1,10-phenanthroline (phen), 1,10-phenanthroline-5,6-dione, 2,9-dimethyl-1,10-phenanthroline-5,6-dione, 2,3-naphthalenediamine, 1,2-diaminobenzene, and ethylene diamine were purchased from Sigma-Alrich and used without further purification. $[Ru(bpy)_2Cl_2]\cdot 2H_2O$ and precursor complexes of other coligands $[Ru(LL)_2Cl_2]$,[26] $[Os(bpy)_2Cl_2]$,[27] benzo[*i*]dipyrido-[3,2-*a*:2′,3′-*c*]phenazine (dppn) and 3,6-dimethyl-dppn (dm-dppn),[23] dipyrido[3,2-a:2′,3′-*c*]phenazine (dppz),[28] and dipyrido-[3,2-d:2′,3′-*f*]-quinoxaline (dpq)[29] were prepared according to known procedures. The purified complexes were isolated as PF_6^- salts and subsequently subjected to anion metathesis on Amberlite IRA-410 with methanol to yield the more water-soluble Cl^- salts for biological experiments.

Characterized fetal bovine serum (FBS) and Iscove's modified Dulbecco's medium (IMDM) supplemented with 4 mM L-glutamine

dx.doi.org/10.1021/ic5002368 | Inorg. Chem. 2014, 53, 4548−4559

were purchased from Fisher Scientific, and human promyelocytic leukemia cells (HL-60) were procured from the American Type Culture Collection. Prior to use, FBS was divided into 40 mL aliquots that were heat inactivated (30 min, 55 °C) and subsequently stored at −20 °C. Plasmid pUC19 DNA was purchased from New England BioLabs and transformed using NovaBlue Singles Competent Cells purchased from Novagen. Transformed pUC19 was purified using the QIAprep Spin Miniprep Kit purchased from Qiagen (yield ∼62 μg of plasmid DNA per 20 mL culture). Water for biological experiments was deionized to a resistivity of 18 MΩ cm using a Barnstead filtration system.

2.2. Instrumentation. Synthetic preparations using microwave irradiation were carried out in a CEM Discover microwave reactor. NMR spectra were collected using a 300 MHz Bruker BZH 300/52 spectrometer at Acadia University's Center for Microstructural Analysis (ACMA), and ESI mass spectra were obtained using a Bruker microTOF focus mass spectrometer from the Maritime Mass Spectrometry Laboratories at Dalhousie University. UV−vis absorption spectra were collected using a Jasco V-530 (Easton, MD, US) spectrophotometer, and singlet oxygen phosphorescence spectra were collected using a custom built version of PTIs QuantaMaster (London, ON, Canada) equipped with a Hamamatsu NIR PMT. An LED array (625 nm, average irradiance 27 ± 2 mW cm^{-2}), manufactured by Fenol Farm, Inc. (Mt. Uniacke, NS, Canada), served as a single-wavelength red light source for the PDT experiments.

2.3. Synthesis. Ruthenium(II) complexes **1**−**10** (Charts 1 and 2) were synthesized according to modified literature protocols using microwave irradiation at 180 °C for 10 min and characterized by TLC, ^{1}H NMR, and mass spectrometry: **1**−**4**,[23,30−32] **6**,[33] **7**,[34] **9**,[35] and **10**.[25] ^{1}H NMR spectra were collected on PF_6^- salts in CD_3CN, and ESI (+ve) mass spectra were run on PF_6^- or Cl^- salts in acetonitrile or methanol, respectively.

Chart 1. Molecular Structures of Ruthenium(II) Complexes 1−4

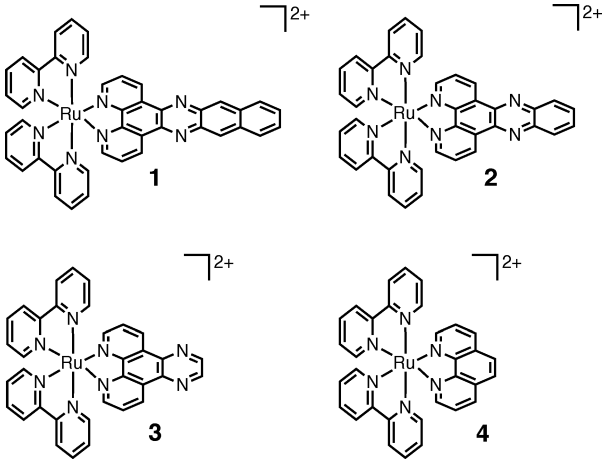

Chart 2. Molecular Structures of Ruthenium(II) Complexes 5−10

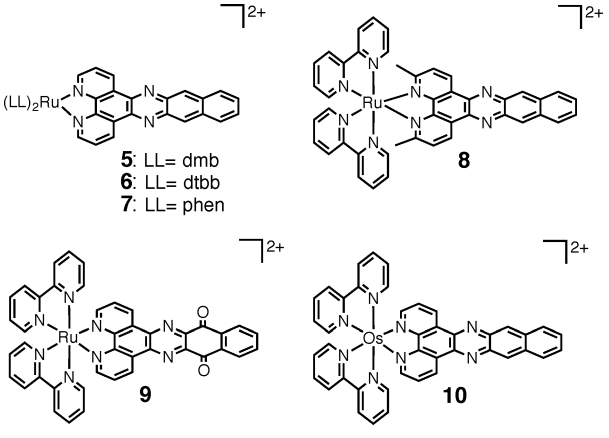

To our knowledge complexes **5** and **8** have not been reported previously. These compounds were prepared by combining Ru(4,4′-dmb)$_2$Cl$_2$ or Ru(bpy)$_2$Cl$_2$ (0.10 mmol) and dppn or dm-dppn (0.10 mmol) in a microwave pressure vessel containing argon-purged ethylene glycol (3.0 mL). The mixture was subjected to microwave irradiation at 180 °C for 10 min. The resulting dark red solution was diluted with water and then washed with dichloromethane to remove residual ligand. Saturated KPF_6 was added dropwise (1−2 mL) to the remaining aqueous phase until no more precipitate formed. The product was then extracted into dichloromethane and evaporated under reduced pressure to give a red solid. The crude material was purified on silica, eluting with 7.5% H_2O in MeCN with 0.5% saturated aqueous KNO_3 to give pure product as a mixture of PF_6^- and NO_3^- salts which were subsequently dissolved in H_2O with sonication. The desired PF_6^- salt was precipitated with saturated KPF_6, extracted into dichloromethane, and concentrated under reduced pressure to give the product as a pure salt which was converted to the water-soluble chloride salt on Amberlite IRA-410 anion exchange resin.

[Ru(dmb)$_2$(dppn)](PF$_6$)$_2$ (**5**) characterization details follow: 57 mg, 66%. R_f ∼ 0.45 in 7.5% H_2O/MeCN, 0.5% saturated KNO3(aq). ^{1}H NMR [CD_3CN]: δ 9.63 (d, 2H, J = 7.11 Hz, c), 9.14 (s, 2H, d), 8.38 (m, 6H, 3,3′,e), 8.14 (d, 2H, J = 4.26 Hz, a), 7.86 (t, 2H, J = 6.76 Hz, b), 7.77 (dd, 2H, J_1 = 3.27 Hz, J_2 = 3.18 Hz, f), 7.64 (d, 2H, J = 5.67 Hz, 6), 7.57 (d, 2H, J = 5.76 Hz, 6′), 7.30 (d, 2H, J = 5.01 Hz, 5), 7.10 (d, 2H, J = 5.22 Hz, 5′), 2.57 (s, 6H, 4), 2.48 (s, 6H, 4′). MS (ESI +) m/z: 837.2 [M − Cl]$^+$, 401.1 [M − 2Cl]$^{2+}$. HRMS (ESI+) m/z for $C_{46}H_{36}N_8Ru$: calcd 401.1048, found 401.1060.

[Ru(bpy)$_2$(dm-dppn)](PF$_6$)$_2$ (**8**) characterization details follow: 71.8 mg, 67%. R_f ∼ 0.45 in 7.5% H_2O/MeCN, 0.5% saturated KNO_3(aq). ^{1}H NMR (CD_3CN): δ 9.67 (d, 2H, J = 9.18 Hz; c), 9.12 (s, 2H, d), 8.53 (d, 2H, J = 7.98 Hz, 3), 8.46 (d, 2H, J = 8.13 Hz, 3′), 8.37 (q, 2H, J = 3.03 Hz, e), 8.03 (m, 4H, J = 8.22 Hz, 4,4′), 7.75 (m, 8H, 5,6,b,f), 7.31 (m, 4H, J = 5.88 Hz, 5′,6′), 2.13 (s, 6H, a). MS (ESI +) m/z: 387.1 [M − 2PF$_6$]$^{2+}$, 919.2 [M − PF$_6$]$^+$. HRMS ESI (+) m/z for $C_{44}H_{32}N_8Ru$: calcd 387.0891, found 387.0908.

2.4. Cell Culture. HL-60 human promyelocytic leukemia cells (ATCC CCL-240) were cultured at 37 °C under 5% CO_2 in RPMI 1640 (Mediatech Media MT-10-040-CV) supplemented with 20% FBS (PAA Laboratories, A15-701) and were passaged 3−4 times per week according to standard aseptic procedures. Cultures were started at 200 000 cells mL^{-1} in 25 cm^2 tissue culture flasks and were subcultured when growth reached 800 000 cells mL^{-1} to avoid senescence associated with prolonged high cell density. Complete media was prepared in 200 mL portions as needed by combining RPMI 1640 (160 mL) and FBS (40 mL, prealiquoted and heat inactivated), in a 250 mL Millipore vacuum stericup (0.22 μm) and filtering.

2.5. Cytotoxicity and Photocytotoxicity Assays. Experiments were performed in triplicate in 96-well microtiter plates (Corning Costar, Acton, MA), where outer wells along the periphery contained 200 μL pH 7.4 phosphate buffered saline (PBS) with 2.68 mM potassium chloride, 1.47 mM potassium phosphate monobasic, 0.137 M sodium chloride, and 8.10 mM sodium phosphate dibasic to minimize evaporation from sample wells. HL-60 cells growing in log phase (approximately 8 × 10^5 cells) were transferred in 50-μL aliquots to inner wells containing warm culture medium (25 μL) and placed in a 37 °C, 5% CO_2 water-jacketed incubator (Thermo Electron Corp., Forma Series II, model 3110, HEPA class 100) for 1 h to equilibrate. Ruthenium compounds were serially diluted with PBS and prewarmed before 25-μL aliquots of the appropriate dilutions were added to the cells and incubated at 37 °C under 5% CO_2 for drug-to-light intervals of 1 or 16 h. Untreated microplates were maintained in a dark incubator while PDT-treated microplates were irradiated in one of the following ways: visible light (400−700 nm, 27.8 mW cm^{-2}) using a 190 W BenQ MS510 overhead projector; red light (625 nm, 28.7 mW

dx.doi.org/10.1021/ic5002368 | Inorg. Chem. 2014, 53, 4548−4559

cm^{-2}) from an LED array; or filtered light from a 600 W Bell & Howell model 301 transparency projector with Edmund Optics 4 × 5" optical cast plastic filters in place. The power densities of blue (#43941), green (#43935), red (#43947), and IR (#43954) color-filtered light were 91.2, 84.2, 93.5, and 85.5 mW cm^{-2}, respectively. Irradiation times from these light sources were approximately 60, 58, and 18−20 min, respectively, in order to yield light doses of ∼100 J cm^{-2}. Variable energy densities (Table 1) were obtained by systematically reducing the irradiation time using the red LEDs. Both dark and PDT-treated microplates were incubated for another 48 h at which point prewarmed, 10-μL aliquots of Alamar Blue reagent (Life Technologies DAL 1025) were added to all sample wells and allowed to incubate for 15−16 h at 37 °C under 5% CO_2. Cell viability was determined on the basis of the ability of the Alamar Blue redox indicator to be metabolically converted to a fluorescent dye by live cells. Fluorescence was quantified with a Cytofluor 4000 fluorescence microplate reader with the excitation filter set at 530 ± 25 nm and emission filter set at 620 ± 40 nm. EC_{50} values for cytotoxicity and photocytotoxicity were calculated from sigmoidal fits of the dose response curves using Graph Pad Prism 6.0 according to eq 1, where y_i and y_f are the initial and final fluorescence signal intensities. For cells growing in log phase and of the same passage number, EC_{50} values were reproducible to within ±25% in the submicromolar regime; ± 10% below 10 μM; and ±5% above 10 μM.

Table 1. Photodynamic Activities of PSs in HL-60 Cells with Four Different Doses of Red Light (625 nm) Delivered at 16 h Drug-to-Light Intervals[a]

	5 J cm^{-2}		25 J cm^{-2}		50 J cm^{-2}		100 J cm^{-2}	
compd	EC_{50} (μM)	PI	EC_{50} (μM)	PI	EC_{50} (μM)	PI	EC_{50} (μM)	PI
1	34	4.0	9.3	15	1.7	81	1.5	91
5	17	6.1	11	9.4	1.9	54	1.9	54
6	4.4	10	2.5	17	1.0	42	0.4	105
7	28	4.9	11	12	2.1	65	1.9	72
8	4.5	13	1.2	50	1.4	43	0.8	75

[a] EC_{50} values refer to light cytotoxicities.

$$y = y_i + \frac{y_i - y_f}{1 + 10^{(\log EC_{50} - x) \times (\text{Hill slope})}} \quad (1)$$

2.6. DNA Photocleavage Assays. DNA photocleavage experiments were performed according to a general plasmid DNA gel mobility shift assay[18,36,37] with 20 μL total sample volumes in 0.5 mL microfuge tubes. Transformed pUC19 plasmid (129 ng in 1.6 μL, >95% Form I) was added to 10 μL of 10 mM Tris-HCl buffer supplemented with 100 mM NaCl (pH 7.5). Serial dilutions of the Ru(II) compounds (0.4, 10, 20, 30, and 40 μM) were prepared in ddH_2O and added in 5-μL aliquots to the appropriate tubes to yield final PS concentrations of 0.1, 2.5, 5.0, 7.5, 10 μM, respectively, and deionized H_2O was added to bring the final assay volumes to 20 μL. Sample tubes were kept at 37 °C in the dark or irradiated. PDT treatments employed either red LEDs (625 nm, 27.7 mW cm^{-2}) or filtered light with power densities of 137, 125, 136, and 128 mW cm^{-2} for blue, green, red, and near-IR, respectively. Irradiation times ranged from 120 min for the red LEDs to 24−26 min for filtered light in order to yield energy densities of approximately 200 J cm^{-2}. After PDT treatment, all samples (dark and light) were quenched by the addition of 4 μL gel loading buffer (0.025% bromophenol blue, 40% glycerol), loaded onto 1% agarose gels cast with 1× TAE (40 mM Tris-acetate, 1 mM EDTA, pH 8.2) containing ethidium bromide (0.75 μg mL^{-1}) and electrophoresed for 30 min at 80 V cm^{-1} in 1× TAE. The bands were visualized with UV-transillumination (UVP transilluminator) and processed using the Gel Doc-It Imaging system (UVP) and the GNU Image Maniupulation Program (GIMP).

2.7. Spectroscopy. Spectroscopic measurements were conducted on dilute (10^{-6}−10^{-5} M) solutions (unless otherwise noted) in spectroscopic-grade water (Cl salts) or acetonitrile (PF_6 salts). Absorption spectra were recorded with a Jasco V-530 spectrophotometer, and singlet oxygen phosphorescence was measured on a PTI Quantamaster equipped with a Hamamatsu R5509-42 NIR PMT for measuring near-infrared (NIR) emission (<1400 nm). Singlet oxygen quantum yields (Φ_Δ) were estimated relative to $[Ru(bpy)_3](PF_6)_2$ (Φ_Δ = 0.57 in aerated acetonitrile).[38]

3. RESULTS AND DISCUSSION

Turro and coworkers pioneered the idea that Ru(II) and Os(II) complexes of dppn with low-lying ^{3}IL states, acting as DNA photocleavers, might play an important role as PSs for PDT and previously demonstrated this concept using tridentate ligands of pydppn complexed to Ru(II) to generate singlet oxygen with unity efficiency.[20] Recently, we reported that PEP complexes, also characterized by low-lying ^{3}IL states, are very potent *in vitro* PDT agents.[10] This work followed an earlier report that the perdeutero analogues of these systems could photocleave DNA efficiently, even in the absence of oxygen, which led to effective *in vitro* PDT.[18] In order to better understand our own systems based on the PEP ligand, we prepared the published dppn complex **1** as well as several derivatives to probe the versatility of ^{3}IL states for PDT. We were particularly interested in whether these extremely photosensitizing ^{3}IL configurations could transform traditional blue-green absorbing PSs into agents that respond to wavelengths of light in the PDT window (600−850 nm).

3.1. Photodynamic Activity. In this study, we used a human leukemia cancer cell line (HL-60) and the Alamar Blue (AB) cell viability test to quantify the *in vitro* PDT effect for a series of complexes derived from the π-expansive dppn ligand. The HL-60 cell line is a standard model used[10,18,39] to probe photodynamic activity by PSs in live cells. HL-60 cells were dosed with PS concentrations of 1 nM to 300 μM (the upper limit due to solubility constraints) and assessed following an incubation period. The baseline (dark) cytotoxicity (total incubation time t = 80 h) associated with compound **1**, reported as the effective concentration to reduce cell viability by 50% (EC_{50}), varied from 250 μM at early passages (n < 10) to an average of 136 μM at mid passages (n = 20−25) and down to 97 μM when cells began to show significant morphological changes (n = 30). This increase in cytotoxicity with time-in-culture was expected given the documented variation of drug cytotoxicity with cell passage number[40] and necessarily leads to differences in calculated values for the phototherapeutic index [PI = EC_{50} (dark)/EC_{50} (light)] of a PS as a function of n. For consistency, our reported dose−response curves were collected on midpassage cells growing in log phase except for the data shown in Figure 1, which was collected on early passage cells growing in log phase. For *in vitro* PDT experiments, drug-to-light intervals (t_{hv}) were either 1 or 16 h, and post-PDT treatment incubation times were approximately 63 h with Alamar Blue added at 48 h. Therefore, total incubation times post-PS delivery were 65 or 80 h, determined by t_{hv}. PDT treatments were carried out with 3 different light sources: white light from a 190 W projector (27.8 mW cm^{-2}), filtered light from a 600 W projector (84.2−93.5 mW cm^{-2}), or red light from a high-power LED array (28.7 mW cm^{-2}) for the appropriate time to achieve the desired fluence. With an energy density of 100 J cm^{-2} and t_{hv} = 16 h, light EC_{50} values for compound **1** were as small as 0.5 μM (PI = 274) with white light treatment and still over twice as potent as the dark treatment with filtered near-IR light (EC_{50} = 102 μM, PI = 2.5).

dx.doi.org/10.1021/ic5002368 | Inorg. Chem. 2014, 53, 4548−4559

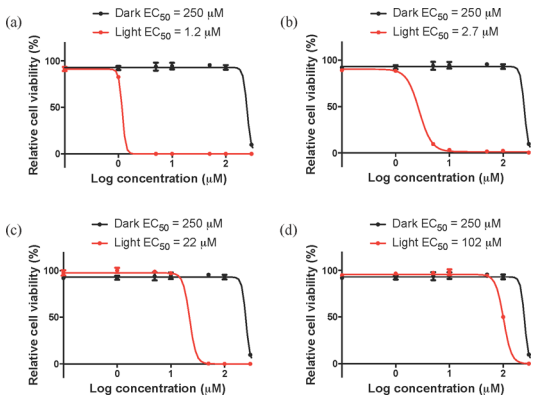

Figure 1. *In vitro* multiwavelength PDT dose–response curves for complex **1** in HL-60 cells: (a) blue, (b) green, (c) red, and (d) NIR light. PDT-treated samples were irradiated with 100 J cm^{-2} of long-pass filtered light (t_{hv} = 16 h).

3.1.1. Multiwavelength PDT with ^{3}IL States. The one-photon wavelength dependence of PDT is well-known, and it can be predicted that PDT efficiency will attenuate as molar extinction coefficients (ε) become smaller as a function of wavelength. For blue/green-absorbing PSs such as compound **1**, visible light absorption peaks in the blue (420 nm, ε = 15 000 M^{-1} cm^{-1}) and diminishes by 7-, 160-, and 750-fold in the green (530 nm, ε = 2170 M^{-1} cm^{-1}), red (625 nm, ε = 93 M^{-1} cm^{-1}), and near-IR (750 nm, ε = 20 M^{-1} cm^{-1}), respectively. The trend in Ru(II) complexes derived from less π-expansive ligands (**2** and **3**) is similar, but absorption past 600 nm is negligible (Figure 2); thus, no red PDT effect should be

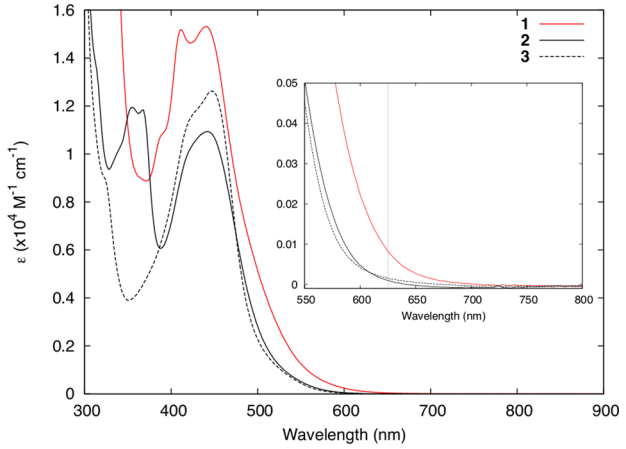

Figure 2. Electronic absorption spectra of complexes **1**–**3** ([PS] = 100 μM, Beer's law obeyed) at room temperature in aqueous buffer (5 mM Tris/50 mM NaCl, pH 7.4). Inset: expanded view with ε_{625} marked.

observed. Despite the marginal red absorption that dppn imparts to its Ru(II) complexes, it would not be expected that ε values <100 M^{-1} cm^{-1} will lead to a PDT effect in cells unless the photosensitizing excited state is extraordinarily efficient.

Turro reported the excited state lifetime of compound **1** to be 33 μs[23] (deoxygenated CH_3CN) by transient absorption spectroscopy, and assigned this lowest lying, nonemissive state as ^{3}IL in nature. The long lifetime in hypoxia and low radiative rate (k_r) of this dppn-centered state signal the absence of efficient, internal excited state deactivation pathways that would otherwise compete with photosensitization processes. Consequently, excited state quenching of these states by external species such as molecular oxygen is facile, and as a result, ^{3}IL states exhibit extreme sensitivity to oxygen and other reactive agents.[10,41] Their enhanced photosensitizing efficiency make these dppn-based systems excellent candidates for multi-wavelength PDT using PS activation wavelengths characterized by notably small ε.

Figure 1 offers proof-of-concept that *in vitro* multiwavelength PDT is possible with PSs that do not have high absorption cross sections in the red or near-IR. Using compound **1** as a prototype PS with excited state dynamics dominated by a long-lived ^{3}IL state, we assessed the photodynamic effect in cells using blue, green, red, and near-IR long-pass-filtered incandescent light at a total fluence of 100 J cm^{-2}. As expected, **1** was most phototoxic when blue wavelengths were included in the light dose (Figure 1a), yielding an EC_{50} value of 1.2 μM and PI > 200. As the shorter blue and green wavelengths of light were filtered (Figure 1b,c), the EC_{50} values increased to 2.7 and 22 μM, respectively. It was striking to us that red/near-IR light activation of **1** produced toxicities an order of magnitude greater than its baseline, dark cytotoxicity, maintaining a sizable therapeutic window even when the number of absorbed photons was extremely low ($\varepsilon \ll 100$ M^{-1} cm^{-1}). This observation was especially encouraging given that activation with long-pass filtered red/near-IR light represents a lower limit in terms of phototherapeutic potential. Considering 650–850 nm to be the PDT window, wavelengths that penetrate tissue most effectively, red long-pass-filtered excitation blocks almost 50% of the incident light at 650 nm and 25% at 675 nm. In other words, of the 100 J cm^{-2} energy density delivered to the PS, the usable range may have been much less than 50% and the optimal range even smaller. With near-IR filtered light, **1** was still almost 2.5× more toxic over the dark control when more than 60% of exciting light ≲700 nm was blocked (Figure 1d).

While it might be surprising to discern this magnitude of activity with a PS that does not absorb red or near-IR light, Sadler and coworkers[42] have reported similar anomalies, whereby DNA photoadduct formation can be induced with low-power red laser light (647 nm, ≈15 mW) for platinum complexes with very low absorbance at this wavelength (ε_{647} < 10 M^{-1} cm^{-1}). In systems where low-lying ^{3}IL excited states are implicated in highly efficient photosensitizing processes, the photobiological activity induced with activation wavelengths of low ε is less puzzling. In our experiments, thermal effects from the irradiation source have been ruled out as contributing factors given that not all PSs exhibit the effect. To understand better the factors that influence long-wavelength PDT with low-lying ^{3}IL excited states in nominally blue-green absorbing PSs, we proceeded to document *in vitro* PDT in a series of related dppn-based complexes. For this investigation, we employed single-wavelength red LEDs emitting at 625 nm as the light source in order to eliminate artifacts related to broadband excitation.

3.1.2. Single-Wavelength, Red PDT with ^{3}IL States. HL-60 cells growing in log phase at midpassage were used to assess red PDT induced by **1** at two different drug-to-light intervals in comparison to PDT with unfiltered white light. As shown in Figure 3, the dark EC_{50} recorded for **1** was 136 ± 1 μM, approximately 1.8× more cytotoxic than that measured against cells of early passage number. With white-light PDT, a short drug-to-light interval (t_{hv} = 1 h) resulted in an EC_{50} value of 1.2 μM while a relatively long drug-to-light interval (t_{hv} = 16 h)

dx.doi.org/10.1021/ic5002368 | Inorg. Chem. 2014, 53, 4548–4559

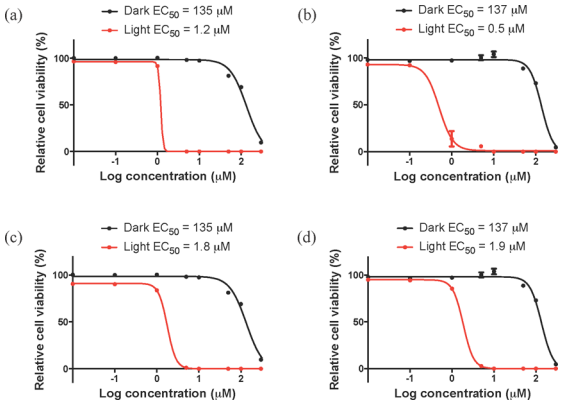

Figure 3. *In vitro* PDT dose–response curves for complex **1** in HL-60 cells. Dark (black) and light (red) conditions were identical except that the PDT-treated samples were irradiated with 100 J cm^{-2} of white light (a, b) or red light (c, d). Drug-to-light intervals were 1 h (a, c) or 16 h (b, d).

yielded almost 2.5× greater toxicity (EC_{50} = 0.5 μM), placing the photobiological activity of compound **1** in the nanomolar regime with a therapeutic index of ~275.

This potency is on par with the photodynamic activity reported for PSs derived from PEP ligands that possess low-lying ^{3}IL excited states with unprecedented photosensitizing capacity,[10] which exceeds some of the largest reported PIs to date.[39] We conclude that ^{3}IL excited states of microsecond-lifetime could be considered a general approach in the design of universally potent PSs for photodynamic applications. It follows that ligands based on PEP and dppn, and certainly other motifs that lead to ligand-centered excitons, are well-suited to function at low oxygen tension and may tolerate a wide range of *in vivo* conditions.

Importantly, the light cytotoxicity measured for compound **1** did not change substantially when 100 J cm^{-2} of red light (625 nm) was used as the PDT treatment instead of broad-band white light (Figure 3c, Table 2). Red PDT with **1** was not as sensitive to the drug-to-light interval since the light EC_{50} changed from only 1.8 to 1.9 μM on going from t_{hv} = 1 to 16 h (Figure 3d). The differential sensitivities of the light EC_{50} values in response to t_{hv} between white-light PDT and red PDT, though not fully understood, underscores the importance of the light treatment in what should be recognized as a combination therapy. At 625 nm the molar extinction coefficient of **1** was 92.7 M^{-1} cm^{-1}, yet PIs for single-wavelength, red PDT at this wavelength were as large as 75 even at short drug-to-light intervals. The cytotoxicity of **1** with red-light activation was as potent as Photofrin but with a therapeutic index almost 30 times greater, owing to the significant dark toxicity associated with this clinical agent (Photofrin dark EC_{50} = 5.34 μM).[43] We make this comparison between **1** and the clinically approved, porphyrin-based PS only to highlight the potential of these transition metal PSs with long-lived ^{3}IL states; at this time, we are focused on optimization of the new PSs prior to undertaking systematic comparisons with clinical PDT agents.

Table 2. Photodynamic Index (PI) of 1 in HL-60 Cells Measured under Two Different Light Doses and Two Different Drug-to-Light Intervals[a]

	light treatment 100 J cm^{-2}	
drug-to-light interval (h)	white	red (625 nm)
1	113 (1.2 μM)	75 (1.8 μM)
16	274 (0.5 μM)	72 (1.9 μM)

[a]PI is the ratio of dark to light toxicity and reflects the effective PDT range of the PS. Numbers in parentheses are light cytotoxicities reported as EC_{50} values from fits of dose–response curves.

For red-absorbing Ru(II)-based DNA photobinders derived from 2,2′-biquinoline, it takes roughy 6.5× the absorbing power of the PS to yield PIs in the 3–20 range with relatively long t_{hv}.[44] While these two classes of PSs operate via entirely different PDT mechanisms, the comparison is made to draw attention to the unique opportunity afforded by ^{3}IL states to expand the repertoire of PSs that can be used for red PDT. In other words, the power of blue-green absorbing PSs to elicit red PDT should not be overlooked, especially when ^{3}IL-based excited states are invoked.

3.1.3. ^{3}IL States Are Required for Red PDT. Complexes **2**–**4** (Chart 1) were prepared in order to ascertain the importance of ^{3}IL states in eliciting the red PDT effect. Like **1**, complex **2** is a strong DNA intercalator owing to the large π-surface dppz ligand, but unlike **1**, its excited state dynamics are dictated by short-lived (τ = 750 ns, deaerated MeCN),[45] lowest-lying ^{3}MLCT states that produce the well-known DNA light-switch effect.[34] Compounds **3** and **4**, based on dpq and phen ligands, respectively, also have lowest-lying ^{3}MLCT states but with truncated π-networks that do not intercalate DNA strongly. The relatively short lifetimes of **2**–**4** in comparison to **1** point toward fairly efficient internal deactivation pathways that compete effectively with external photosensitizing processes. From structure–photophysics relationships, it is evident that the phenazine-fused benzene ring along the coordination axis of the dppn ligand is necessary to drop the energy of the ^{3}IL state well below that of the lowest-lying ^{3}MLCT states.[25] Figure 4 clearly shows that this structural feature and the resulting low-energy ^{3}IL state is an absolute requirement for *in vitro* red PDT. The EC_{50} value measured for compound **1** using a different batch of midpassage HL-60 cells produced a slightly higher light toxicity (EC_{50} = 1.5 μM) with no significant change to dark toxicity (PI = 91). With 100 J cm^{-2} of red light (625 nm), compounds **2**–**4** produced no discernible photodynamic activity (PI ≈ 1).

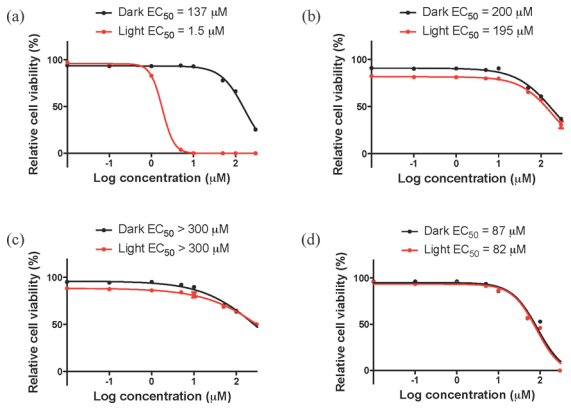

Figure 4. *In vitro* PDT dose–response curves for complexes **1** (a), **2** (b), **3** (c), and **4** (d) in HL-60 cells. PDT-treated samples were irradiated with 100 J cm^{-2} of red light (625 nm) with a drug-to-light interval of 16 h.

dx.doi.org/10.1021/ic5002368 | *Inorg. Chem.* 2014, 53, 4548–4559

3.1.4. Scope of Red PDT with ^{3}IL States. If red PDT is a general phenomenon associated with blue-green absorbing PSs possessing low-lying, long-lived ^{3}IL states, then the number of PSs belonging to this class should be correspondingly broad. The use of modular architectures presented by tris-bidentate or bis-tridentate Ru(II) scaffolds affords the ability to fine-tune certain properties while maintaining a potent PDT effect. Using compound **1** as the parent, one can envision subtle modifications to the ancillary ligands that will alter the overall lipophilicity of the complex and thereby affect cellular uptake and subcellular localization. Such changes can be exploited to optimize the relative dark and light cytotoxicities, in search of larger therapeutic windows and nanomolar potencies.

Substitution of the bpy coligands in **1** with dmb, dtbb, or phen (**5**–**7**, respectively) gave rise to compounds that were all capable of sensitizing red PDT, with light EC_{50} values under 2 μM. As expected, the dark toxicities varied with the identity of the coligand, providing a means to change the therapeutic window substantially: PIs ranged from 50 to over 100. Figure 5

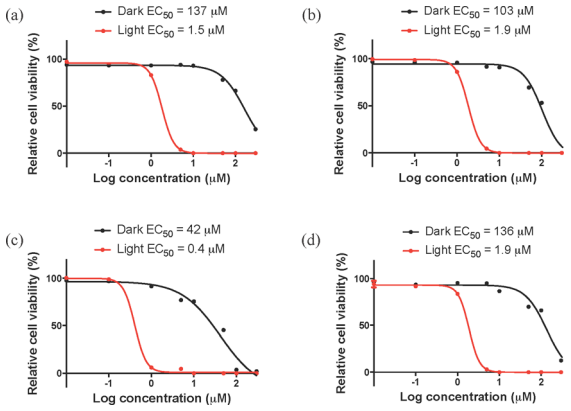

Figure 5. *In vitro* PDT dose–response curves for complexes **1** (a), **5** (b), **6** (c), and **7** (d) in HL-60 cells. PDT-treated samples were irradiated with 100 J cm^{-2} of red light (625 nm) with a drug-to-light interval of 16 h.

demonstrates that red PDT is a general phenomenon across a variety of coligands but that certain changes lead to particularly effective PSs. For example, incorporation of *t*-butyl groups at the 4,4′ positions of bipyridyl ancillary ligands led to a light toxicity of 400 nM and a PI of 105 while dmb or phen coligands (in **5** and **7**) produced less potent PSs and smaller PIs relative to **1** but still 50–70× more potent than dark controls. Given that ε_{625} for complexes **1** and **5**–**7** did not parallel the magnitudes of their light EC_{50} values, we infer that red PDT is not controlled by subtle differences in the absorption spectra of these compounds but by other photophysical and photobiological factors.

To probe whether ^{3}IL excited states dominate the photobiological activity of dppn-based Ru(II) complexes when low-lying, ligand-dissociative ^{3}MC (triplet metal-centered) become thermally accessible from ^{3}MLCT states, we introduced potential disruptions to the coordination sphere in the form of bulky methyl groups at positions 3 and 6 on the dipyridyl rings (**8**). Glazer and coworkers have shown that strained Ru(II) complexes produced by bulky groups in the coordination sphere of diimine ligands[39,46] and by steric clash of long-axis extended ligands[44] act as phototriggered DNA-metalating agents and make excellent oxygen-independent PSs for *in vitro* PDT. In contrast to Glazer's $[Ru(bpy)_2(dmdppz)]^{2+}$ (dmdppz = 3,6-dimethyldipyrido[3,2-a:2′,3′-*c*]phenazine),[46] compound **8** did not photoeject the crowded dppn ligand. This inability to form a ligand-deficient, reactive metal center upon photoexcitation suggests that the presence of a long-lived, low-lying ^{3}IL state prevents access to the stabilized ^{3}MC states that result from structural distortion.[47] Figure 6b shows that the

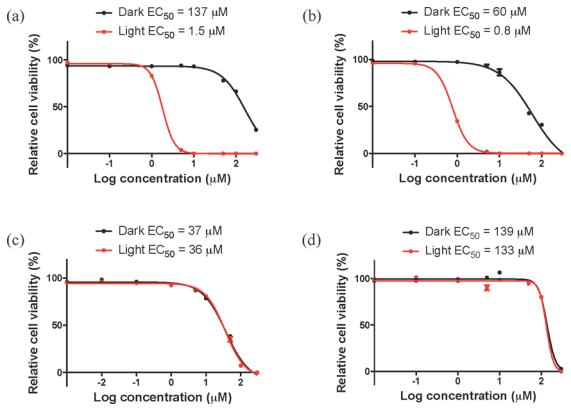

Figure 6. *In vitro* PDT dose–response curves for complexes **1** (a), **8** (b), **9** (c), and **10** (d) in HL-60 cells. PDT-treated samples were irradiated with 100 J cm^{-2} of red light (625 nm) with a drug-to-light interval of 16 h.

light toxicity for red PDT by compound **8** was submicromolar, with a respectable therapeutic window (PI = 75). We infer that peripheral substitutions on the dppn ligand at less-compromising positions will also be well-tolerated. The ability to maintain excited state dynamics dictated by low-lying ^{3}IL states despite structural changes to both the coligand set and to dppn itself demonstrates the generality of these ligand-centered states for red PDT. Their collective potency is underscored by the marked light EC_{50} values and corresponding PIs that are maintained even with red light doses as low as 5 J cm^{-2} (Table 1). Thus, it should be possible, from the vast number of combinations, to optimize further the red and near-IR PDT with blue/green-absorbing PSs.

To ascertain whether intracellular photodecomposition of the complexed dppn ligand[33] was responsible for this phenomenon of red PDT in some way, we photooxidized **1** with 420 nm light (7.36 mW cm^{-2}) over 45 h in the presence of oxygen to obtain **9** in high purity after column chromatography. As expected, this oxidation of the phenazine unit of dppn obliterated the PDT effect with red light and increased HL-60 cytotoxicity by almost 4-fold (Figure 6c). Compound **9** did not yield red PDT or PDT at any wavelength employed, including broad-spectrum white light (100 J cm^{-2}, 1- or 16-h drug-to-light intervals). This inactivity underscores that compound **9** is characterized by fundamentally different excited states in comparison to **1** and **5**–**8**. Efficient quenching of the excited state(s) in **9** has previously been ascribed to intramolecular photoinduced electron transfer (PET) mediated by the quinone fragment,[48,49] and our results are consistent with an excited state of very short duration.

Photooxidation of **8** was also accomplished, surprisingly, with no competing photoejection despite the known tendency of 2,9-dimethyl-substituted phenathroline-based ligands to photoeject with modest light exposure.[39,46] The oxidized derivative of **8** also did not produce PDT in HL-60 cells under any of our conditions and was more cytotoxic than **8**. Therefore, it appears to be a general observation that photodecomposition products

dx.doi.org/10.1021/ic5002368 | *Inorg. Chem.* 2014, 53, 4548–4559

of compounds containing dppn are inactive for PDT and thus do not explain the red PDT effect. It should be noted that compounds **1** and **5**−**8** were entirely stable to the light fluences employed in the present multiwavelength PDT experiments.

3.1.5. Limitations of Red PDT with ^{3}IL States. Turro outlined a Jabłonski diagram for $[Os(bpy)_2(dppn)]^{2+}$ (**10**) and compared its photophysical scheme to that of compound **1** (Figure 7). Both complexes possess lowest-lying ^{3}IL states, but

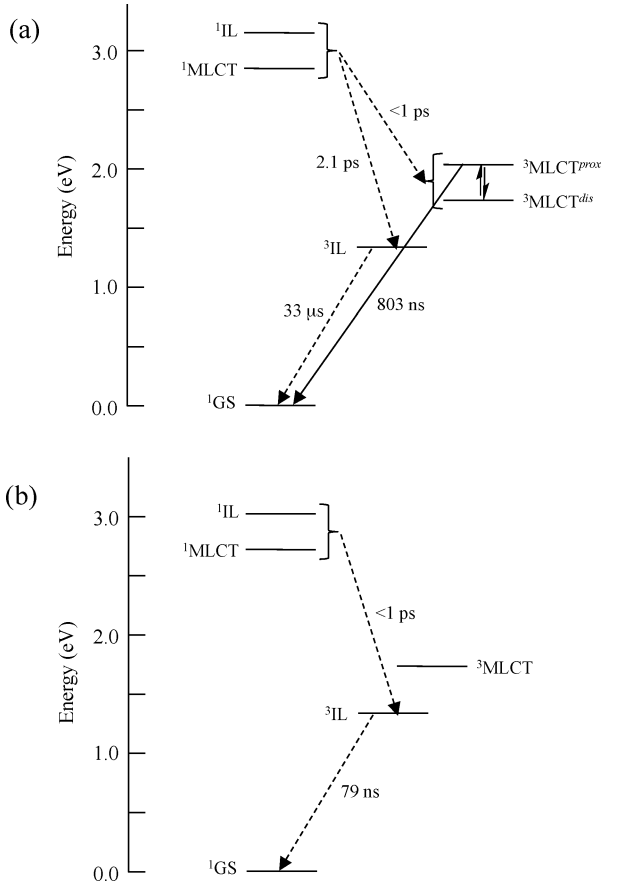

Figure 7. Jabłonski diagrams of compounds **1** (a) and **10** (b) in CH_3CN, with lifetimes and energies from refs 23 and 25.

the lifetime of this state in the Os(II) congener is only 79 ns, over 3 orders of magnitude less than that for **1**.[23,25] If the long lifetimes of ^{3}IL states are primarily responsible for conferring the highly efficient photosensitizing capacity that makes red PDT possible at wavelengths of low ε, then compound **10** provides a convenient test of this theory since its lifetime is significantly shortened due to increased spin−orbit coupling to the ground state and possible configuration mixing with the ^{3}MLCT state. Complex **10** was completely inactive in our *in vitro* red PDT experiments (Figure 6d) yet was over 30 times more absorptive at 625 nm (Figure 8, Table 3). We corroborated this observation by assaying the related $[Os(LL)_2(dmdppn)]^{2+}$ and $[Os(LL)_2(dppns)]^{2+}$ complexes (analogues of **5**−**8** where LL = dmb, dtbb, and phen) and found no PDT effect with red light. Therefore, we conclude that while the existence of low-lying ^{3}IL states appears to be a prerequisite for red PDT, the lifetimes of these states must be suitably long to ensure red photodynamic effects. Contrary to what has been proposed,[25] the increased red absorption cross sections that characterize Os(II) complexes (ε_{625} = 3130 M^{-1} cm^{-1}) do not

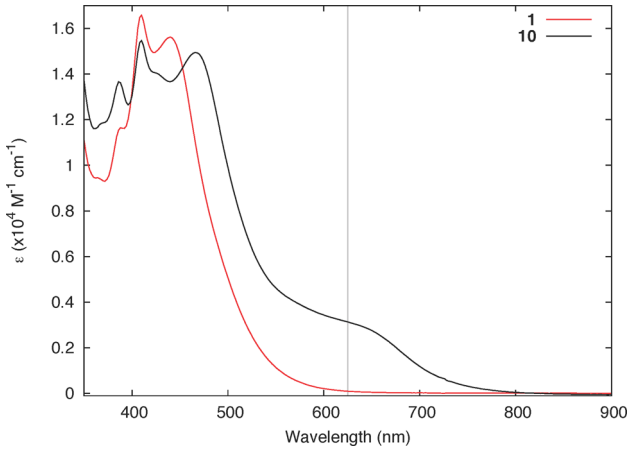

Figure 8. Electronic absorption comparison of complexes **1** and **10** ([PS] = 20 μM) in aqueous buffer (5 mM Tris/50 mM NaCl, pH 7.4). Vertical line represents LED excitation wavelength (625 nm).

Table 3. *In Vitro* Red PDT (625 nm, 100 J cm^{-2}) in HL-60 Cells with a Drug-to-Light Interval of 16 h

	red PDT (100 J cm^{-2})		
compd	light EC_{50} (μM)	PI	ε (M^{-1} cm^{-1})[a](625 nm)
1	1.5	91	92.7
2	195	~1	0[b]
3	>300	~1	0[b]
4	82	~1	0[b]
5	1.9	54.2	289
6	0.4	105	401
7	1.9	71.6	119
8	0.8	75.6	198
9	36	~1	58.6
10	133	~1	3130

[a]Extinction coefficients were reproducible to within ±10 M^{-1} cm^{-1}. [b]No signal detected at 20 μM PS; signal <10 M^{-1} cm^{-1} at 100 μM PS.

lead to red PDT when the lowest-lying excited states are ^{3}IL in origin. However, white-light PDT with compound **10** was marginally effective (light EC_{50} = 15 μM, PI = 9.3), presumably due to fractional population of low-energy ^{3}MLCT states that sensitize $^1O_2$ with shorter wavelengths of light.

3.2. DNA Photocleavage. To establish that the red photodynamic activity was not an artifact of the cellular environment (i.e., due to sensitization by a metabolic product of the PS or by sensitization of another cellular agent), we employed a DNA photocleavage assay as a means to probe the ability of the complexes to photodamage biological macromolecules in response to red light activation in a cell-free environment. Figure 9 shows the dose−response profile of **1** for phototriggered damage to pUC19 plasmid DNA (20 μM bases) when activated with blue, green, red, and near-IR light, respectively. Lanes 1−2 and 8 are controls, and demarcate mostly undamaged, supercoiled DNA (form I). Compound **1** induced single-strand breaks in plasmid DNA, resulting in the slower-migrating, nicked circular DNA (form II), at concentrations of 1−10 μM and PS-to-nucleotide ratios (r_b) as low as 0.1, with wavelengths of light from blue to near-IR. The magnitude of DNA photodamage as a function of wavelength can be seen clearly in lane 4 (2.5 μM **1**, r_b = 0.125), where blue light was most effective (100% conversion from form I to nicked form II). Notably, significant potency was maintained

dx.doi.org/10.1021/ic5002368 | Inorg. Chem. 2014, 53, 4548−4559

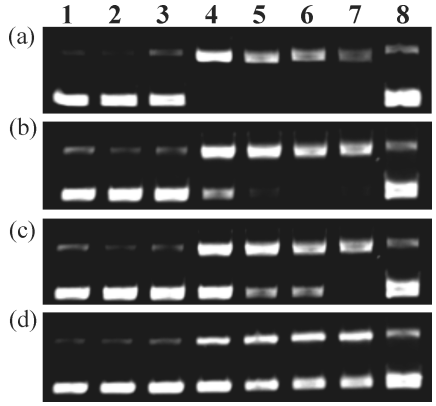

Figure 9. DNA photocleavage of pUC19 plasmid (20 μM bases) dosed with compound **1** and 200 J cm^{-2} of (a) blue (>400 nm), (b) green (>450 nm), (c) red (>600 nm), or (d) near-IR (>650 nm) light. Gel mobility shift assays employed 1% agarose gels (0.75 μg mL^{-1} ethidium bromide) electrophoresed in 1× TAE at 8 V cm^{-1} for 30 min. Lane 1, DNA only ($-h\nu$); lane 2, DNA only ($+h\nu$); lane 3, 1.0 μM **1** ($+h\nu$); lane 4, 2.5 μM **1** ($+h\nu$); lane 5, 5.0 μM **1** ($+h\nu$); lane 6, 7.5 μM **1** ($+h\nu$); lane 7, 10 μM **1** ($+h\nu$); and lane 8, 10 μM **1** ($-h\nu$).

using both red and near-IR light (Figure 9c,d). Red light produced 100% form II at 10 μM **1** (r_b = 0.5) while near-IR retained ~50% activity relative to blue-light activation under these conditions. The photodynamic activity of **1** in cell-free media using plasmid DNA as a biological probe paralleled the *in vitro* multiwavelength PDT we measured in HL-60 cells (Figure 1) for this light-responsive agent. Therefore, we conclude that the red PDT effect we observe in both cells and cell-free media is induced by blue-green absorbing PSs and their highly photosensitizing ^{3}IL states rather than by a metabolic or photodecomposition byproduct(s).

We reconfirmed this assertion by assaying the DNA photobiological activity associated with complexes whose excited state dynamics are controlled by lowest-lying ^{3}MLCT states. As was the case for the *in vitro* red PDT experiments, reference compounds **2**–**4** did not damage DNA even when activated with 200 J cm^{-2} of filtered red light or with the same dose of single-wavelength red light (Figure 10). The photoreactivity observed for **1** was similar, 100% conversion from

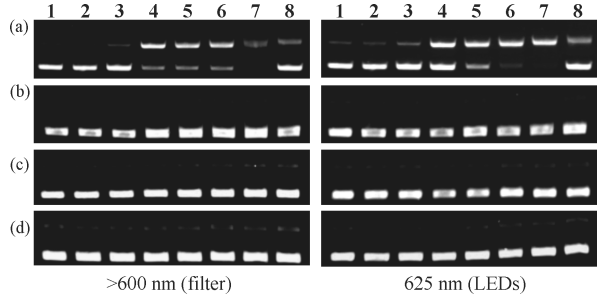

Figure 10. DNA photocleavage of pUC19 plasmid (20 μM bases) dosed with compound **1** (a), **2** (b), **3** (c), or **4** (d) and 200 J cm^{-2} of filtered (left panel) or single-wavelength (right panel) red light. Gel mobility shift assays employed 1% agarose gels (0.75 μg mL^{-1} ethidium bromide) electrophoresed in 1× TAE at 8 V cm^{-1} for 30 min. Lane 1, DNA only ($-h\nu$); lane 2, DNA only ($+h\nu$); lane 3, 1.0 μM PS ($+h\nu$); lane 4, 2.5 μM PS ($+h\nu$); lane 5, 5.0 μM PS ($+h\nu$); lane 6, 7.5 μM PS ($+h\nu$); lane 7, 10 μM PS ($+h\nu$); and lane 8, 10 μM PS ($-h\nu$).

form I to form II at r_b = 0.5, regardless of the source of red light employed. The DNA photobiological profiles of compounds **9** and **10** also mirrored the *in vitro* red PDT outcomes in HL-60 cells (Figure 11). The absence of DNA photodamage with red

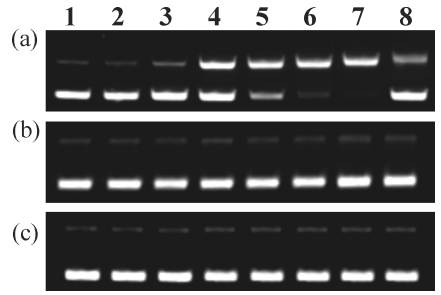

Figure 11. DNA photocleavage of pUC19 plasmid (20 μM bases) dosed with compound **1** (a), **9** (b), or **10** (c), and 200 J cm^{-2} of single-wavelength LED light (625 nm). Gel mobility shift assays employed 1% agarose gels (0.75 μg mL^{-1} ethidium bromide) electrophoresed in 1× TAE at 8 V cm^{-1} for 30 min. Lane 1, DNA only ($-h\nu$); lane 2, DNA only ($+h\nu$); lane 3, 1.0 μM PS ($+h\nu$); lane 4, 2.5 μM PS ($+h\nu$); lane 5, 5.0 μM PS ($+h\nu$); lane 6, 7.5 μM PS ($+h\nu$); lane 7, 10 μM PS ($+h\nu$); and lane 8, 10 μM PS ($-h\nu$).

light by **9** and **10** reaffirms the importance of the benzo[*i*]-phenazine-fused skeleton for establishing low-lying ^{3}IL excited states and that these states must have suitably long lifetimes in order to showcase a highly efficient photodynamic potency in both cells and cell-free media. Apparently, τ = 79 ns in **10** is too short to harness the potential of ^{3}IL states for PDT.

A small amount of DNA cleavage was initiated by compound **1** in the dark (lane 8 in Figures 9–11). Highly purified plasmid DNA preparations typically carry up to 5% damaged DNA, which can be discerned as the baseline level of form II in both control and reaction lanes. Of the dark reaction lanes, only those containing **1** showed some damage above this threshold, and the effect was marginal (≤10%). Few examples of DNA cleavage by Ru(II) complexes in the absence of co-oxidants, redox-active metals, or photons exist. However, hydrogen bonding to the phosphodiester backbone by Ru(II)-bound bipyridine-glycoluril units has been successfully exploited for hydrolytic cleavage without the addition of external agents.[50] We are unsure whether the phenazine skeleton of dppn could play a similar role, but if so, its contribution is minor. Attempts to probe this dark DNA damage by compound **1** with simple gel electrophoresis at higher concentrations of PS were thwarted by the disappearance of bands, which often happens as a result of interference with ethidium bromide binding or quenching of ethidium bromide emission.

3.3. Singlet Oxygen Sensitization. The quantum yield for $^1O_2$ production by compound **1** in cell-free media with λ_{ex} = 420 nm was 81% relative to $[Ru(bpy)_3]^{2+}$ as the standard, which is reported as 56% in aerated MeCN.[38] Due to the long lifetimes of Ru(II)-derived ^{3}IL states and their energetic proximities to singlet oxygen, type II photosensitization processes should remain notably efficient even when the effective concentration of molecular oxygen is very low.[20−23] However, despite this ability to sensitize $^1O_2$ under very low oxygen concentrations, this mechanism alone cannot explain the high *in vitro* potency achieved with these systems, which surpasses what is documented for similar PSs that operate exclusively via a $^1O_2$ mechanism. Indeed, the potency cannot be explained by activity of ROS generally. This raises the

dx.doi.org/10.1021/ic5002368 | Inorg. Chem. 2014, 53, 4548−4559

important question of the mechanism of cell damage by these long-lived ^{3}IL states. It has been proposed that compound **1** acts as a dual type I/II agent against pUC18 plasmid DNA in a cell-free environment since DNA photodamage was observed in hypoxia.[23] Consequently, type I, oxygen-independent processes will likely be invoked in cells as well, and the relative importance of oxygen versus oxygen-independent PDT will be influenced by the (i) PS concentration, (ii) wavelength(s) of light employed, (iii) light fluence and irradiance, and importantly (iv) intracellular targets and the availability and identity of nearest reacting sensitization mediators.

Due to the low absorption of red and near-IR wavelengths of light, the quantity of $^1O_2$ generated by **1** with 625 nm excitation was far less than what was produced with 450 nm excitation (Figure 12). Interestingly, despite sufficient energy to sensitize

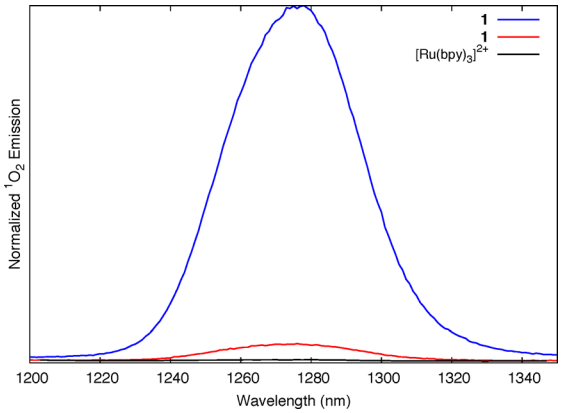

Figure 12. Singlet oxygen phosphorescence sensitized by complex **1** with 450 nm excitation (blue) and with 625 nm excitation (red). Lack of $^1O_2$ sensitization by $[Ru(bpy)_3]^{2+}$ with 625 nm excitation (black) included for comparison.

singlet oxygen from the lowest-lying ^{3}IL state with red-light excitation, the $^1O_2$ quantum yield measured for compound **1** was wavelength dependent, with almost negligible $^1O_2$ production using 625 nm excitation. However, red PDT with **1** was extremely effective, with light EC_{50} values as low as 1.5 μM and PIs greater than 90. For some derivatives of **1**, namely **6**, nanomolar light toxicities were measured with similarly low values for Φ_Δ. From this data, we infer that type I photoprocesses may be the major contributors to the PDT effect, especially when longer wavelengths of light are employed. The high potency of these PSs even with minimal absorption of red light also suggests that PSs operating via type I mechanisms may be significantly better than those that utilize type II mechanisms in that the striking photobiological efficiency of the former would be expected to tolerate more compromising conditions *in vivo*.

3.4. ^{3}IL Excited State Reactivity. Turro and co-workers reported that compound **1** photocleaves DNA with $\lambda_{irr} \geq 550$ nm via mechanisms that do not depend exclusively on $^1O_2$ and other ROS.[23] From $E_{00} \sim 2.1$ eV and $E_{1/2}([Ru]^{2+/+}) = -0.46$ V, it was concluded that an excited state reduction potential (E^*_{red}) of ~1.64 V versus NHE was sufficient to photooxidize guanine (+1.29 vs NHE at pH 7).[51] Stern–Volmer quenching of the weak ^{3}MLCT emission by GMP, analogous to $[Ru(hat)_3]^{2+}$ (hat = 1,4,5,8,9,12-hexaazatriphenylene) with a similar excited state reduction potential,[52] provided convincing evidence of type I photoreactivity via direct oxidation of guanine. Therefore, it was proposed that compound **1** acts as a dual type I/II agent that employs its reactive ^{3}MLCT state for direct guanine photooxidation and its ^{3}IL state for $^1O_2$ sensitization. Together, this combined action from both states was postulated to be the factor responsible for high reactivity.

In the previous account, compound **1** did not photocleave DNA with $\lambda_{irr} \geq 645$ nm,[23,25] and from this, we infer that the unreported energy and power densities were relatively small. In our experiments, 200 J cm^{-2} with $\lambda_{irr} \geq 650$ nm photocleaved DNA with 50% conversion of form I to form II at the highest concentration of PS tested (10 μM, $r_b = 0.5$). Moreover, the photobiological activity toward DNA observed for compound **1** and its derivatives **5**–**8** translated to *in vitro* multiwavelength PDT and, notably, PDT with red and near-IR light. While smaller red and near-IR light doses, e.g., ≤5 J cm^{-2}, did not produce notable DNA photodamage in the gel electrophoretic titrations, these reduced energy densities did lead to *in vitro* PDT with light EC_{50} values as low as 4.4 μM with a 10-fold therapeutic margin over dark cytotoxicity (Table 1).

The PS activation schemes employed in our biological studies used 625 (1.98 eV) and ≥650 nm (≤1.91 eV) irradiation. Both methods provide sufficient energy for direct population of thermalized ^{3}IL states (estimated at 1.5 eV,[20] calculated at 1.34[21]), but not enough energy to achieve substantial population of thermalized ^{3}MLCT states, estimated at 2.10 eV from the emission maximum of **1** and theoretical calculations.[21,23] The photophysical trajectory put forward by Turro (Figure 7a) argues against population of the lower-lying ^{3}IL state from the more energetic ^{3}MLCT state. If this premise holds, then it follows that higher photon energy blue PDT will utilize both ^{3}MLCT and ^{3}IL states in type I and II photoprocesses, respectively, and red/near-IR PDT will harness only ^{3}IL reactivity through presumably type II mechanisms. The drastically reduced $^1O_2$ quantum yield on going from blue to red excitation juxtaposed with the pronounced red and near-IR PDT in cells complicates this picture and warrants further investigation given that these low energies were not previously thought to invoke type I photooxidation of guanine. It is possible that nonthermalized ^{3}IL states could play a role in this chemistry or that previous estimates and calculations of the thermalized ^{3}IL state energies are underestimated. Type I photoprocesses other than direct DNA oxidation may also be important. It should be noted that these scenarios do not take into account photothermal effects (release of PS vibrational energy as heat) that could be operative *in vivo*.[53]

4. CONCLUDING REMARKS

While there is immense interest in exploiting the attractive photophysical and photochemical properties of transition metal complexes for photobiological applications such as PDT, no such agents have been approved for clinical use. A perceived obstacle is the inability of most transition metal complexes to sensitize singlet oxygen or other reactive species in the PDT window, where porphyrin-based PSs offer a key advantage. However, the drawbacks associated with clinically approved, organic PSs and the inherent problems with *in vivo* dosimetry warrant continued effort toward the development of metal–organic agents that have the potential to afford unprecedented versatility as PSs. For example, panchromatic activation and dual type I/II photoswitching would broaden the scope of PSs for PDT, opening up the possibility of using a single PS in a wide variety of clinical situations, whereby light is used to tune the activity of the PS for a particular tumor type or phenotype.

dx.doi.org/10.1021/ic5002368 | Inorg. Chem. 2014, 53, 4548–4559

In lieu of truly panchromatic absorbers with respectable extinction coefficients and PDT potency from UV to near-IR, we show that highly photosensitizing ^{3}IL excited states can offset the low extinction coefficients associated with most transition metal complexes in the PDT window. Given that Ru(II)-based systems can be designed to include both photooxidizing ^{3}MLCT states and $^1O_2$-sensitizing ^{3}IL states, type I/II photoswitching has already been accomplished by us and others. In the present study, we highlight not only that this dual activity can be controlled by the light treatment employed but also that PSs that have been previously overlooked as PDT agents should be re-examined. Blue-green absorbing Ru(II) complexes derived from π-expansive ligands with microsecond lifetimes can be activated with red and near-IR light to yield PSs for multiwavelength PDT. Importantly, we document that compounds **1** and **5**−**8** are highly potent PSs, with light EC_{50} values of 0.4−1.9 μM, that act in the PDT window with very low extinction coefficients. Their light EC_{50} values meet or surpass those of Photofrin, and the PI ratios are superior to this clinical agent.[43] These findings represent the first steps toward improving the performance and versatility of PSs for better *in vivo* dosimetry. Efforts are underway to understand the wavelength-dependent photophysics and ensuing PDT for these metal complexes, and to optimize the light treatment for near-IR PDT.

■ ASSOCIATED CONTENT

Supporting Information

Structure numbering of compounds **5** and **8** used for ^{1}H NMR proton assignments. This material is available free of charge via the Internet at http://pubs.acs.org.

■ AUTHOR INFORMATION

Corresponding Author

*E-mail: sherri.mcfarland@acadiau.ca.

Notes

The authors declare no competing financial interest.

■ ACKNOWLEDGMENTS

We thank the Natural Sciences and Engineering Research Council of Canada, the Canadian Institutes for Health Research, the Canadian Foundation for Innovation, and the Nova Scotia Research and Innovation Trust for financial support and Professor Todd Smith for use of his cell and tissue culture facility. We also thank Professor Douglas Magde (UCSD) and Professor Edith Glazer (UK Lexington) for insightful discussions regarding the work described in this Article.

■ REFERENCES

(1) Bonnett, R. *Chemical Aspects of Photodynamic Therapy*; Gordon and Breach Science Publishers: London, 2000.

(2) Bown, S. G. *J. Natl. Compr. Cancer Network* **2012**, *10* (Suppl 2), S69−74.

(3) Plaetzer, K.; Krammer, B.; Berlanda, J.; Berr, F.; Kiesslich, T. *Lasers Med. Sci.* **2009**, *24*, 259−268.

(4) Triesscheijn, M.; Baas, P.; Schellens, J. H. M.; Stewart, F. A. *Oncologist* **2006**, *11*, 1034−1044.

(5) Brown, S. B.; Brown, E. A.; Walker, I. *Lancet Oncol.* **2004**, *5*, 497−508.

(6) Jarvi, M.; Patterson, M.; Wilson, B. *Biophys. J.* **2012**, *102*, 661−671.

(7) Gross, S. A.; Wolfsen, H. C. *Gastrointest. Endosc. Clin. N. Am.* **2010**, *20*, 35−53.

(8) van Veen, R. L. P.; Robinson, D. J.; Siersema, P. D.; Sterenborg, H. J. C. M. *Gastrointest. Endosc.* **2006**, *64*, 786−788.

(9) Weersink, R. A.; Bogaards, A.; Gertner, M.; Davidson, S. R. H.; Zhang, K.; Netchev, G.; Trachtenberg, J.; Wilson, B. C. *J. Photochem. Photobiol., B* **2005**, *79*, 211−222.

(10) Lincoln, R.; Kohler, L.; Monro, S.; Yin, H.; Stephenson, M.; Zong, R.; Chouai, A.; Dorsey, C.; Hennigar, R.; Thummel, R. P.; McFarland, S. A. *J. Am. Chem. Soc.* **2013**, *135*, 17161−17175.

(11) Thompson, M. S.; Johansson, A.; Johansson, T.; Andersson-Engels, S.; Svanberg, S.; Bendsoe, N.; Svanberg, K. *Appl. Opt.* **2005**, *44*, 4023−4031.

(12) Zhu, T. C.; Finlay, J. C. *Med. Phys.* **2008**, *35*, 3127−3136.

(13) Juris, A.; Balzani, V.; Barigelletti, F.; Campagna, S.; Belser, P.; von Zelewsky, A. *Coord. Chem. Rev.* **1988**, *84*, 85−277.

(14) McClenaghan, N. D.; Leydet, Y.; Maubert, B.; Indelli, M. T.; Campagna, S. *Coord. Chem. Rev.* **2005**, *249*, 1336−1350.

(15) Kozlov, D. V.; Tyson, D. S.; Goze, C.; Ziessel, R.; Castellano, F. N. *Inorg. Chem.* **2004**, *43*, 6083−6092.

(16) Goze, C.; Kozlov, D. V.; Tyson, D. S.; Ziessel, R.; Castellano, F. N. *New J. Chem.* **2003**, *27*, 1679−1683.

(17) Simon, J. A.; Curry, S. L.; Schmehl, R. H.; Schatz, T. R.; Piotrowiak, P.; Jin, X.; Thummel, R. P. *J. Am. Chem. Soc.* **1997**, *119*, 11012−11022.

(18) Monro, S.; Scott, J.; Chouai, A.; Lincoln, R.; Zong, R.; Thummel, R. P.; McFarland, S. A. *Inorg. Chem.* **2010**, *49*, 2889−2900.

(19) Ford, W. E.; Rodgers, M. A. J. *J. Phys. Chem.* **1992**, *96*, 2917−2920.

(20) Liu, Y.; Hammitt, R.; Lutterman, D. A.; Joyce, L. E.; Thummel, R. P.; Turro, C. *Inorg. Chem.* **2009**, *48*, 375−385.

(21) Foxon, S. P.; Alamiry, M. A. H.; Walker, M. G.; Meijer, A. J. H. M.; Sazanovich, I. V.; Weinstein, J. A.; Thomas, J. A. *J. Phys. Chem. A* **2009**, *113*, 12754−12762.

(22) Foxon, S. P.; Metcalfe, C.; Adams, H.; Webb, M.; Thomas, J. A. *Inorg. Chem.* **2007**, *46*, 409−416.

(23) Sun, Y.; Joyce, L. E.; Dickson, N. M.; Turro, C. *Chem. Commun.* **2010**, *46*, 2426−2428.

(24) Lei, W.; Zhou, Q.; Jiang, G.; Zhang, B.; Wang, X. *Photochem. Photobiol. Sci.* **2011**, *10*, 887−890.

(25) Sun, Y.; Joyce, L. E.; Dickson, N. M.; Turro, C. *Chem. Commun.* **2010**, *46*, 6759−6761.

(26) Sullivan, B. P.; Salmon, D. J.; Meyer, T. J. *Inorg. Chem.* **1978**, *17*, 3334−3341.

(27) Kober, E. M.; Caspar, J. V.; Sullivan, B. P.; Meyer, T. J. *Inorg. Chem.* **1988**, *27*, 4587−4598.

(28) Dupureur, C. M.; Barton, J. K. *Inorg. Chem.* **1997**, *36*, 33−43.

(29) Collins, J. G.; Sleeman, A. D.; Aldrich-Wright, J. R.; Greguric, I.; Hambley, T. W. *Inorg. Chem.* **1998**, *37*, 3133−3141.

(30) Schatzschneider, U.; Niesel, J.; Ott, I.; Gust, R.; Alborzinia, H.; Wölfl, S. *ChemMedChem.* **2008**, *3*, 1104−1109.

(31) Zhou, Q.-X.; Lei, W.-H.; Chen, J.-R.; Li, C.; Hou, Y.-J.; Wang, X.-S.; Zhang, B.-W. *Chem.—Eur. J.* **2010**, *16*, 3157−3165.

(32) Friedman, A. E.; Chambron, J. C.; Sauvage, J. P.; Turro, N. J.; Barton, J. K. *J. Am. Chem. Soc.* **1990**, *112*, 4960−4962.

(33) Rau, S.; Schwalbe, M.; Losse, S.; Görls, H.; McAlister, C.; MacDonnell, F. M.; Vos, J. G. *Eur. J. Inorg. Chem.* **2008**, *2008*, 10311034.

(34) Hartshorn, R. M.; Barton, J. K. *J. Am. Chem. Soc.* **1992**, *114*, 5919−5925.

(35) Chesneau, B.; Hardouin-Lerouge, M.; Hudhomme, P. *Org. Lett.* **2010**, *12*, 4868−4871.

(36) Croke, D. T.; Perrouault, L.; Sari, M. A.; Battioni, J. P.; Mansuy, D.; Helene, C.; Le Doan, J. *J. Photochem. Photobiol.* **1993**, *18*, 41−50.

(37) Praseuth, D.; Gaudemer, A.; Verlhac, J. B.; Kraljic, I.; Sissoeff, I.; Guille, E. *Photochem. Photobiol.* **1986**, *44*, 717−724.

(38) DeRosa, M. C.; Crutchley, R. J. *Coord. Chem. Rev.* **2002**, *233/234*, 351−371.

(39) Howerton, B. S.; Heidary, D. K.; Glazer, E. C. *J. Am. Chem. Soc.* **2012**, *134*, 8324−8327.
(40) Guo, D.; Zhang, X.; Huang, Z.; Zhou, X.; Zhu, L.; Zhao, Y.; Gu, N. *Sci. China: Life Sci.* **2012**, *55*, 898−905.
(41) Ji, S.; Wu, W.; Wu, W.; Song, P.; Han, K.; Wang, Z.; Liu, S.; Guo, H.; Zhao, J. *J. Mater. Chem.* **2010**, *20*, 1953−1963.
(42) Mackay, F. S.; Woods, J. A.; Heringova, P.; Kasparkova, J.; Pizarro, A. M.; Moggach, S. A.; Parsons, S.; Brabec, V.; Sadler, P. J. *Proc. Natl. Acad. Sci. U.S.A.* **2007**, *104*, 20743−20748.
(43) Berlanda, J.; Kiesslich, T.; Engelhardt, V.; Krammer, B.; Plaetzer, K. *J. Photochem. Photobiol., B* **2010**, *100*, 173−180.
(44) Wachter, E.; Heidary, D. K.; Howerton, B. S.; Parkin, S.; Glazer, E. C. *Chem. Commun.* **2012**, *48*, 9649−9651.
(45) Brennaman, M. K.; Alstrum-Acevedo, J. H.; Fleming, C. N.; Jang, P.; Meyer, T. J.; Papanikolas, J. M. *J. Am. Chem. Soc.* **2002**, *124*, 15094−15098.
(46) Wachter, E.; Howerton, B. S.; Hall, E. C.; Parkin, S.; Glazer, E. C. *Chem. Commun.* **2014**, *50*, 311−313.
(47) Structural distortion is inferred; no X-ray crystallographic data were collected.
(48) Díaz, R.; Francois, A.; Barrera, M.; Loeb, B. *Polyhedron* **2012**, *39*, 59−65.
(49) Kim, M.-J.; Konduri, R.; Ye, H.; MacDonnell, F. M.; Puntoriero, F.; Serroni, S.; Campagna, S.; Holder, T.; Kinsel, G.; Rajeshwar, K. *Inorg. Chem.* **2002**, *41*, 2471−2476.
(50) Deshpande, M. S.; Kumbhar, A. A.; Kumbhar, A. S. *Inorg. Chem.* **2007**, *46*, 5450−5452.
(51) Steenken, S.; Jovanovic, S. V. *J. Am. Chem. Soc.* **1997**, *119*, 617−618.
(52) Lecomte, J.-P.; Kirsch-De Mesmaeker, A.; Feeney, M. M.; Kelly, J. M. *Inorg. Chem.* **1995**, *34*, 6481−6491.
(53) Lim, C.-K.; Shin, J.; Lee, Y.-D.; Kim, J.; Oh, K. S.; Yuk, S. H.; Jeong, S. Y.; Kwon, I. C.; Kim, S. *Theranostics* **2012**, *2*, 871−879.

dx.doi.org/10.1021/ic5002368 | *Inorg. Chem.* 2014, 53, 4548−4559